Theor Chem Acc (2004) 112: 318–326
DOI 10.1007/s00214-004-0591-2

Theoretical
Chemistry Accounts

Regular article

Effects of protonation on proton-transfer processes in guanine–cytosine Watson–Crick base pairs

M. Noguera, M. Sodupe, J. Bertrán

Departament de Química, Universitat Autónoma de Barcelona, Bellaterra, 08193, Spain

Received: 18 September 2003 / Accepted: 18 December 2003 / Published online: 16 June 2004

Abstract. Intermolecular proton-transfer processes in guanine–cytosine Watson–Crick base pairs have been studied using the B3LYP density functional method. Protonation of the base pair was carried out both at the N7 and at the O6 atoms of guanine. It is found that protonation induces a strengthening of the base pair and facilitates the N1–N3 single-proton-transfer reaction. The double-proton-transfer reaction, however, turns out to be unfeasible when the system is protonated at these sites. Mutagenic implications of these proton-transfer processes are discussed.

Keywords: Base pair – DNA – Proton transfer – Mutation – Density functional calculations

Introduction

It has been 50 years since Watson and Crick [1] proposed their double helix model for the three-dimensional structure of DNA, possibly the most important biological macromolecule. Its stability is partially associated with the hydrogen-bond interactions that take place among the different nitrogenated bases, the hydrogen-bonding pattern being determined by the complementarity of their forms. This specificity of recognition between bases is responsible for maintaining the genetic code. Ten years later, Löwdin [2, 3] proposed that intermolecular proton-transfer mechanisms could alter these hydrogen-bonding patterns and ultimately lead, through base-mispairing, to spontaneous mutations. Two cases, which approximately correspond to spontaneous and induced phenomena, were distinguished. The first one referred to pairs of equally charged bases. In this case, concerted double-proton-transfer reactions would take place in order not to create a charge separation. The second one referred to pairs with unequally charged bases generated through the introduction of a negative or a positive charge in one of the bases (e.g., protonation). Under these conditions the probability of single-proton-transfer reactions from the more positively charged moiety to the more negatively charged one would be greatly increased.

For many years it has not been possible to check theoretically Löwdin's suggestions; however, in the last decade, with the development of computers and cost-effective theoretical approaches, many studies related to DNA nucleobases have appeared. Most of them deal with the relative stability of nucleobase tautomers [4–20] or their acid–base properties [9, 21–35]. Studies on proton-transfer processes in base pairs are scarcer [36–43], the single-proton-transfer and double-proton-transfer reactions in pairs of equally charged bases being the processes most often considered [36–38]. Much of the discussion has focused on whether the mechanism of the double-proton-transfer reaction is concerted or stepwise, through a single-proton-transferred ion-pair-like intermediate (Scheme 1). In particular, Florian and Leszczynski [38] studied these processes at the HF/6-31G* level of theory and located an intermediate structure corresponding to the ion-pair species. This structure was found to be about 24 kcal/mol above the neutral form, the transition state of the concerted reaction lying even higher in energy (31 kcal/mol). However, the relative energy of this transition state was significantly decreased (to 14.6 kcal/mol) when performing single-point calculations at the second-order Møller–Plesset perturbation theory (MP2) level. Moreover, at the correlated level, the energy barrier leading to the single-proton-transferred intermediate disappeared, indicating the dubious existence of such an intermediate in this system.

Proceedings of the 11th International Congress of Quantum Chemistry satellite meeting in honour of Jean-Louis Rivail

Correspondence to: J. Bertrán
e-mail: bertran@klingon.uab.es

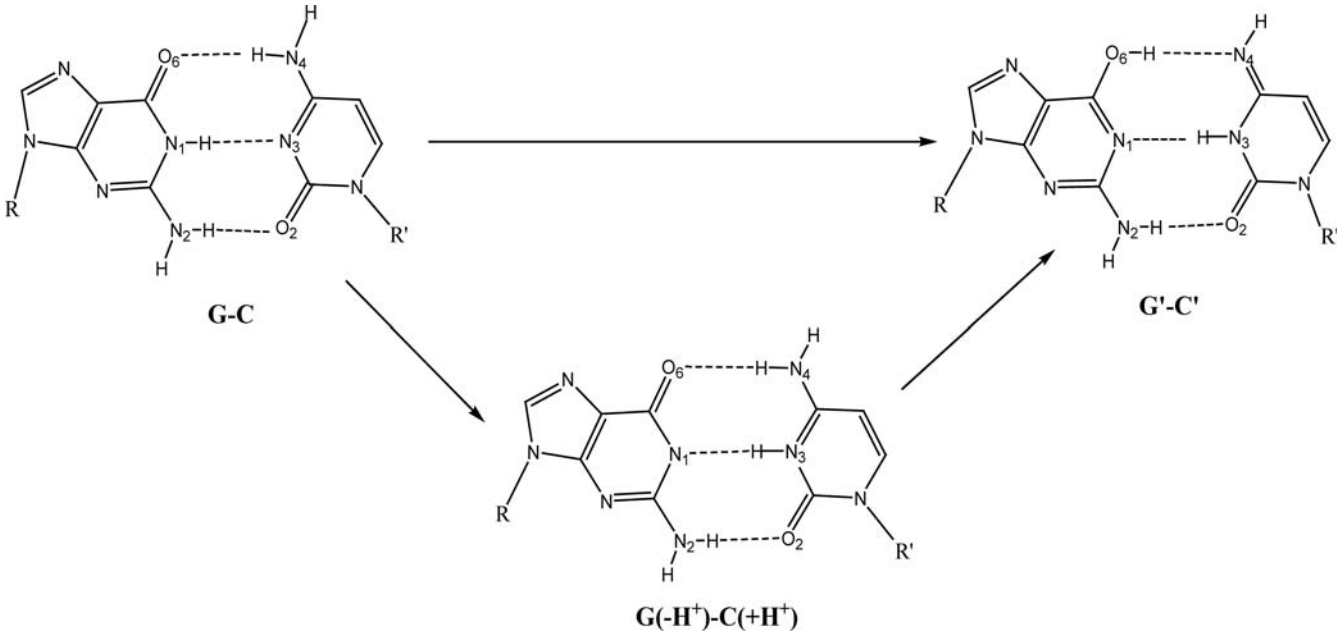

Scheme 1

Less attention has been paid to base pairs with unequally charged bases; i.e., on how the energy profiles of these reactions are modified upon the introduction of a charge in the system. Previous studies on the guanine–cytosine radical cation [39, 40] showed that oxidation of guanine induces a strengthening of the base pair and a stabilization of the single-proton-transferred structure. The double-proton-transferred product, however, was not located as a minimum on the potential-energy surface. Similar results have been reported for the guanine–cytosine radical anion [41].

To our knowledge, the effect of protonating different sites of guanine on these processes has only been considered in one work at the Austin Model 1 (AM1) level [42]. The results showed that protonation easily leads to the single-proton-transferred structure; however, some unexpected results were obtained. On one hand, the double-proton-transferred minimum was also found to be a stable species upon protonation of guanine at the N7 site, in contrast to some preliminary calculations performed in our laboratory at Becke's three-parameter hybrid method with the Lee–Yang–Parr correlation functional (B3LYP) level of theory [43]. On the other hand, a surprisingly bifurcated hydrogen-bonding interaction was observed in guanine–cytosine pair for the O6-protonated system.

In this paper we reexamine the single-proton-transfer and double-proton-transfer reactions in a protonated guanine–cytosine base pair, at the B3LYP level of theory with a double-ζ-quality basis set supplemented with diffuse and polarization functions. Both the N7 and O6 sites of guanine are considered for protonation. Furthermore, solvent effects are estimated through the use of a polarized continuum model (PCM).

Computational details

Full geometry optimizations and frequency calculations for the neutral and the protonated base pairs were performed using the three-parameter B3LYP [44, 45] density functional method as implemented in the Gaussian 98 [46] program package, with the 6-31G(d,p) basis set [47]. The energy values reported in the present work, however, were obtained by performing single-point calculations, at the 6-31G(d,p) optimized geometries, with the larger 6-31 + + G(d,p) basis set. The reliability of density functional methods for studying hydrogen-bonded systems has been analysed in several papers [48, 49], which have shown that nonlocal methods that include gradient corrections, particularly the B3LYP one, provide results comparable to the MP2 method when similar basis sets are used.

The nature of the stationary points was checked by vibrational frequency calculations. Thermodynamic corrections were obtained with the smaller basis set assuming an ideal gas, unscaled harmonic vibrational frequencies and the rigid-rotor approximation by standard statistical methods [50]. Net atomic charges were obtained using the natural population analysis of Weinhold and coworkers [51, 52].

Solvent effects were estimated using the PCM proposed by Miertus and coworkers [53, 54] and Cossi et al. [55] with the large basis set, and considering water as the solvent. These calculations were performed at the gas-phase optimised geometries.

Results and discussion

First, we present the results obtained for neutral guanine–cytosine, G–C. Second, the systems proton-

ated at the N7 and O6 sites of guanine, $H^+G_{N7}C$ and $H^+G_{O6}C$, are considered. In all cases, the single-proton-transfer and double-proton-transfer reactions shown in Scheme 1 were analysed in the gas phase and in solution.

Neutral system

For the neutral system, only the product derived from the double-proton-transfer reaction was found as a minimum on the potential-energy surface. All attempts to optimize the single-proton-transferred ion pair collapsed to the initial nontransferred structure. This fact disagrees with previously published results [38] at the Hartree–Fock level of theory, which characterized the ion-pair structure as a minimum. Therefore, electronic correlation appears to be essential to correctly describe the topology of the potential-energy surface.

The optimized geometries of the neutral system, G–C, the transition state, TS(G–C–G′–C′), and the double-proton-transferred product, G′–C′, are shown in Fig. 1. It is observed that the geometries of the nucleobases themselves remain similar along the process. Only those distances related to the keto-enol and the amino-imino transformation (C–O6, C–N1 and C–N4, C–N3, respectively) change significantly. Hydrogen-bond distances are given in Table 1. It should be mentioned that for G–C, the trends of the computed hydrogen-bond distances differ from the available experimental [56] data, which were obtained from DNA crystals, but agree with other theoretical studies of G–C in the gas phase [39, 40, 57, 58]. As noted previously, the differences are caused by environment effects in the crystal, especially those produced by Na^+ counterions, which have been shown to play a key role in determining hydrogen-bond distances [59].

The double-proton-transfer reaction induces some changes on the hydrogen-bond distances. It can be observed in Table 1 that the O6–N4 and the N1–N3 distances decrease by 0.10 and 0.06 Å, respectively, while the N2–O2 distances increases by 0.07 Å. Such variations mainly result from the changes in the acid–base character of the centres involved in the O6–N4 hydrogen bond. As often observed, hydrogen bonds at the transition structure are shorter than in the reactant or in the product in order to facilitate the proton transfer between heavy atoms.

The energy profile of this process is shown in Fig. 2. It can be observed that the G–C interaction energy is 26.2 kcal/mol. This value is in good agreement with previously published results that include electron correlation [39, 40, 57, 58, 60]. The double-proton-transferred product, G′–C′, lies 9.8 kcal/mol above the reactant species, whereas the energy barrier of the reaction is 14.8 kcal/mol. ΔG_{298} for this double-proton-transfer reaction is 9.8 kcal/mol. The G–C–G′–C′ equilibrium (with a calculated equilibrium constant of 6.2×10^{-8}) will be largely displaced to the reactants and so this double-proton-transfer reaction will occur rarely. Nevertheless, the frequency is still significant from the point of view of the fidelity of DNA replication.

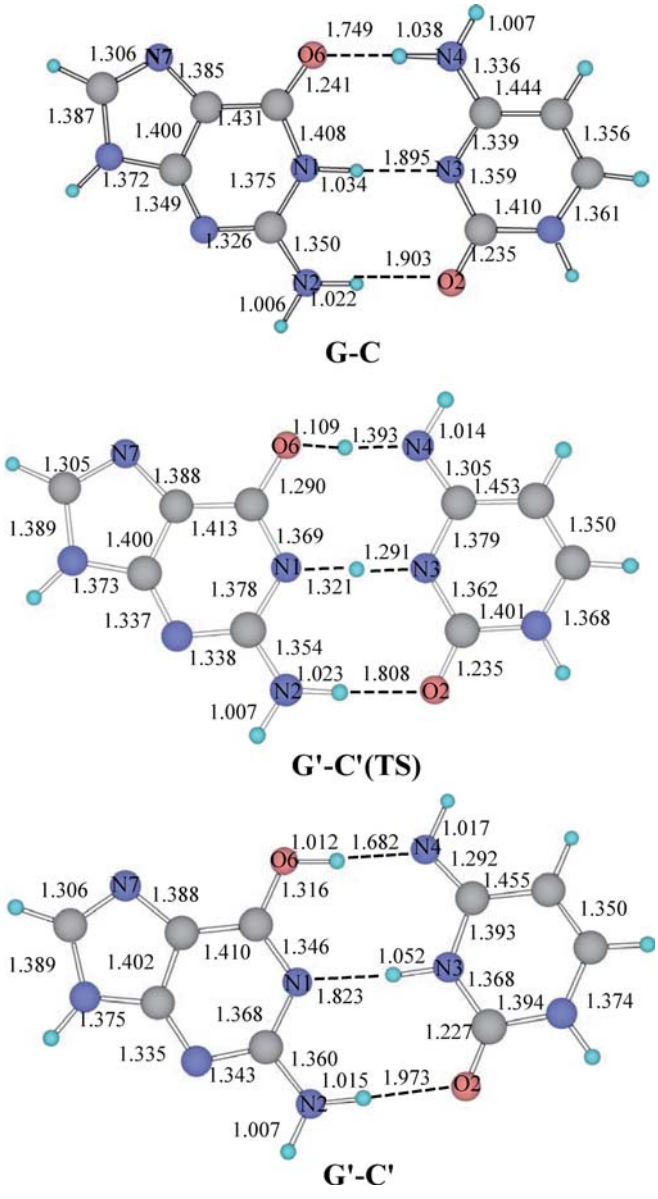

Fig. 1. Optimized geometries for the neutral guanine–cytosine system. Non-proton-transferred (*G–C*), transition-state (*TS*) and double-proton-transferred (*G′–C′*) structures. Distances in angstroms

As mentioned, the ion pair derived from the single-proton-transferred reaction is not found as a minimum on the potential-energy surface. In order to get an

Table 1. Hydrogen-bond distances (Å) for neutral guanine–cytosine base pairs. In *parentheses*, experimental values from crystallographic data [57]

	G–C	TS	G′–C′
O6–N4	2.79 (2.91)	2.50	2.69
N1–N3	2.93 (2.95)	2.61	2.87
N2–O2	2.92 (2.86)	2.83	2.99

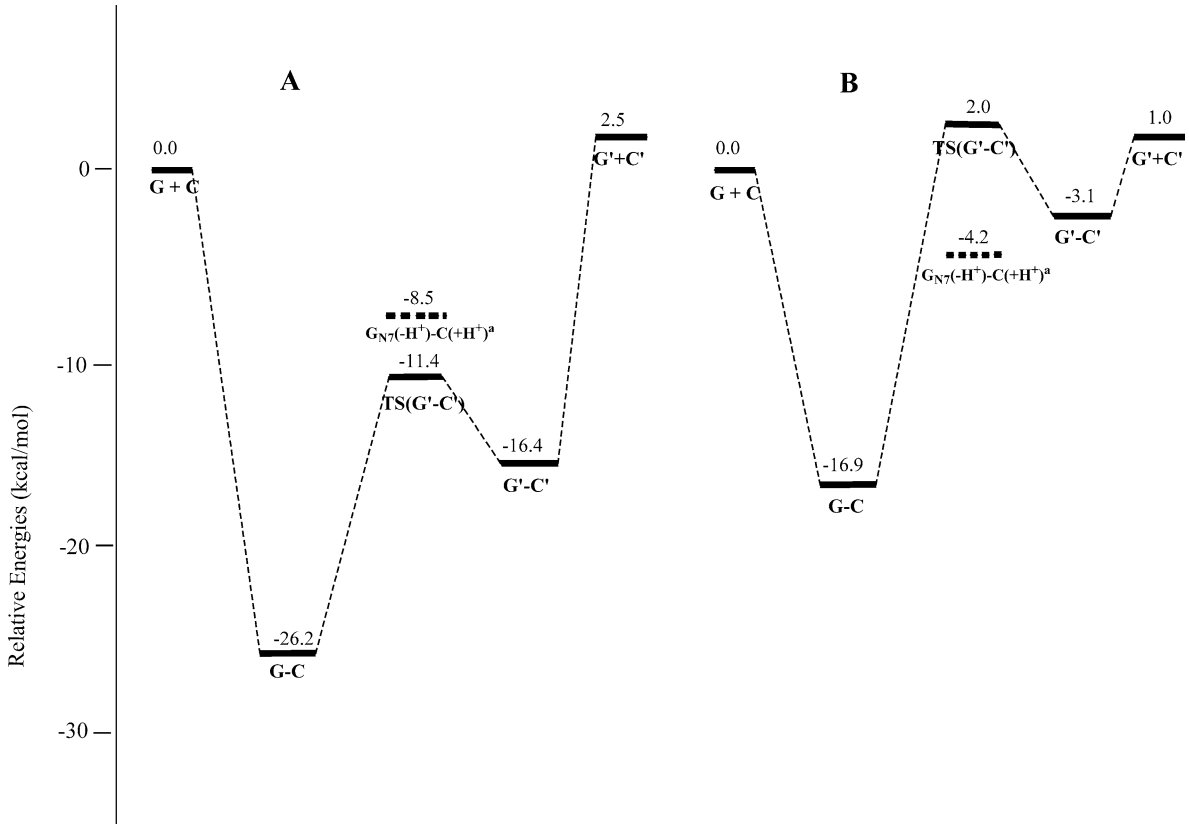

Fig. 2. Energy profile for the double-proton-transfer process in the neutral guanine–cytosine system. *A* In the gas phase, *B* in solution). *Superscript a* indicates that energies were estimated by freezing the N4–H and N3–H distances

estimation of how high in energy this structure lies, we optimized the system with the N3–H and N4–H distances frozen at the values reported by Florián and Leszczynski [38] The structure obtained lies 17.7 kcal/mol above the reactants, in good agreement with single-point calculations at the MP2 level [38]. Natural population analysis shows that the guanine moiety holds a charge of −0.74, while the charge on cytosine is 0.74. Thus, this structure presents important ion-pair character and the solvent may largely stabilize it. Because of that, single-point PCM calculations were carried out for all of the species involved in this process. The results are shown in Fig. 2b. It can be observed that the relative energy of the double-proton-transferred (G′–C′) and the TS(G–C–G′–C′) structures, with respect to G–C, increase by approximately 4 kcal/mol upon including solvent effects. However, the relative energy of the ion-pair structure decreases from 17.7 to 12.7 kcal/mol, this structure now becoming stabler than G′–C′, which suggests that this intermediate may exist in solution and be implied in mutagenic processes.

Protonated systems

The electrostatic potential of the guanine–cytosine base pair depicted in Fig. 3 shows which are the most suitable regions to interact with a positive charge. It can be observed that there is a major region around the N7 and O6 sites of guanine where the electrostatic potential presents the most negative values. Regions around N3 and O2 are far less attractive in this sense. Furthermore, quantum chemical calculations have shown that N7 is the preferred site for protonation followed by O6 [9, 26, 28, 31, 35]. Because of that, these sites are the positions considered for protonation in this work.

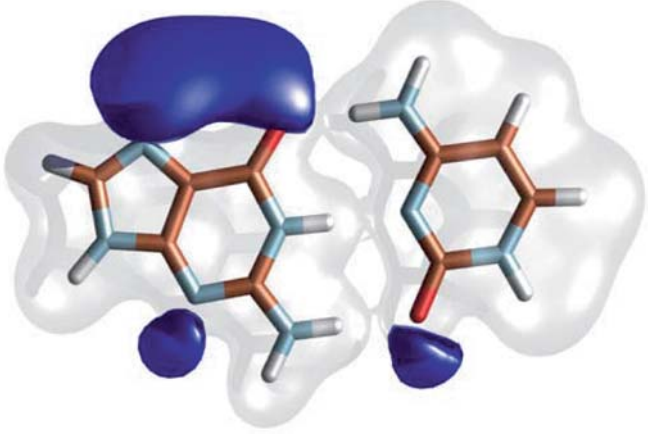

Fig. 3. Electrostatic potential map for the neutral guanine–cytosine base pair. *Dark areas* correspond to negative values

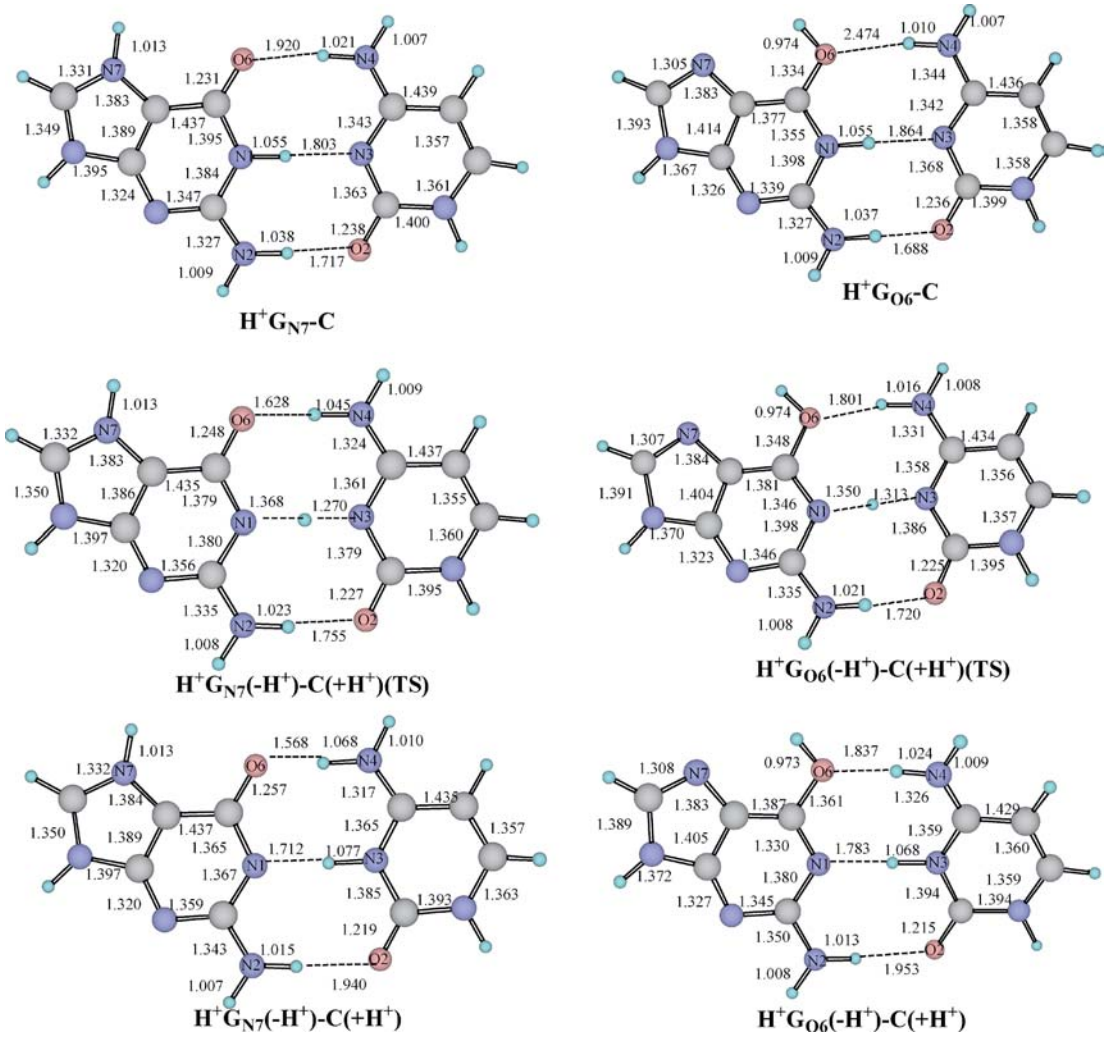

Fig. 4. Geometries for the N7- and O6-protonated systems: non-proton-transferred (H^+G_{N7}–C and H^+G_{O6}–C), TS and single-proton-transferred [$H^+G_{N7}(-H^+)$–$C(+H^+)$ and $H^+G_{O6}(-H^+)$–$C(+H^+)$] structures. Distances in angstroms

In contrast to the neutral system, the double-proton-transferred product was not localized in any case, the optimization process always collapsing to the single-proton-transferred structure, which as we will see later is largely stabilized because of protonation.

The geometries of the two protonated systems, $H^+G_{N7}C$ and $H^+G_{O6}C$, the corresponding transition states and the single-proton-transferred products, $H^+G_{N7}(-H^+)C(+H^+)$ and $H^+G_{O6}(-H^+)C(+H^+)$, are shown in Fig. 4. The major geometrical changes produced by protonation at N7 occur at the five-membered ring. However, for the O6-protonated system the main differences are due to the partial loss of the C = O6 double bond, which causes a strong C–O elongation and a significant shortening of the neighbouring C–C and C–N bonds.

Hydrogen-bond distances for both protonated systems, transition states and single-proton-transferred structures are shown in Table 2. For comparison the distances of the neutral system have also been included. Both for $H^+G_{N7}C$ and $H^+G_{O6}C$, the N1–N3 and N2–O2 hydrogen-bond distances are smaller than in neutral G–C. In contrast, the O6–N4 distance becomes larger in the protonated systems. Variations in the hydrogen-bond distances can be explained considering the acidity changes produced upon protonation. When guanine is

Table 2. B3LYP hydrogen-bond distances (Å) for neutral and N7- and O6-protonated guanine–cytosine base pair

	G–C	H^+G–C		TS		$H^+G(-H^+)$–$C(+H^+)$	
		N_7	O_6	N_7	O_6	N_7	O_6
O6–N4	2.79	2.94	3.48	2.67	2.82	2.64	2.86
N1–N3	2.93	2.86	2.92	2.64	2.66	2.79	2.85
N2–O2	2.92	2.75	2.72	2.78	2.74	2.96	2.97

protonated, its acidity is enhanced, thus promoting the strengthening of hydrogen bonds where guanine acts as the proton donor (i.e., the N1–N3 and N2–O2 bonds). Moreover, protonation decreases the basicity of guanine, which produces a weakening of the hydrogen bond where guanine acts as a proton acceptor (O6–N4 bond).

Hydrogen-bond differences between the two protonation sites are only significant for the O6–N4 distance. This is mainly caused by the fact that O6 protonation transforms the carbonyl oxygen into an enol oxygen, which is less basic. In addition, the electrostatic repulsion between the two hydrogen atoms (the one protonating O6 and the one forming the hydrogen bond) contributes to the weakening of the O6–N4 hydrogen bond. Despite this, the three-hydrogen-bond pattern is retained, in disagreement with the bifurcated structure located with the AM1 method [42]. As found in some cases, the bifurcated structure is probably an artefact of the AM1 method.

In the single-proton-transferred product the charge lies on the cytosine moiety (0.82 and 0.90 for N7 and O6 protonated systems, respectively) and thus hydrogen bonds where cytosine acts as the proton donor are reinforced (O6–N4 and N1–N3), whereas the hydrogen bond where it acts as a proton acceptor is weakened (N2–O2). Hydrogen-bond distances in $H^+G_{O6}(-H^+)C(+H^+)$ are larger than in $H^+G_{N7}(-H^+)C(+H^+)$. Such differences correlate with the $H^+G_{N7}(-H^+)C(+H^+)$ and $H^+G_{O6}(-H^+)$–$C(+H^+)$ interaction energies (see later). Finally, as for the neutral system, the transition structures show smaller hydrogen-bond distances than the corresponding reactants and products.

Base-pair interaction energies for the neutral and protonated systems are shown in Table 3. It can be observed that whereas for G–C, the binding energy (D_e) is 26.2 kcal/mol, for $H^+G_{N7}C$ and $H^+G_{O6}C$ the computed values are 36.7 and 35.5 kcal/mol, respectively. Thus, protonation causes a significant strengthening of the base pair, mainly due to the increase of acidity of guanine. The difference between the D_e values of the two protonation sites is due to the weakening of the O6–N4 hydrogen bond, which is 0.5 Å longer in the O6-protonated system. A simple thermodynamic cycle shows that the increase of the G–C interaction energy (ΔH_{298K}) upon protonation is equivalent to the increase of the proton affinity of guanine associated with base-pairing. That is, the proton affinity at the N7 and O6 sites in the base pair is 14.5 and 9.3 kcal/mol larger, respectively, than that at the same site for guanine alone (Table 3).

The energy profiles are shown in Fig. 5. The major trend that can be observed in these profiles is that the reactant and single-proton-transferred product become much closer in energy than in the case of the neutral system. As shown, the single-proton-transferred structure in the neutral system is estimated to lie about 18 kcal/mol higher in energy than the reactant, whereas for N7- and O6-protonated systems, this species lies only 4.3 and 2.0 kcal/mol higher, respectively. That is, as found previously [42], protonation facilitates enormously the N1–N3 proton transfer and, more importantly, it permits the existence of the single-proton-transferred intermediate. However, the computed B3LYP energy barriers (6.5 and 6.3 kcal/mol) are

Table 3. B3LYP/6-31++G(d,p) interaction energies for neutral, and N7- and O6-protonated guanine–cytosine base pairs (kcal/mol)

	G–C	H^+-G–C	
	Neutral	N_7	O_6
D_e	26.2	36.7	35.5
D_0[a]	24.7	34.8	33.8
$\Delta H^0_{298\,K}$[b]	24.7	35.1	33.9
$\Delta G^0_{298\,K}$[b]	13.2	22.3	22.1

[a]Includes zero-point energy computed from the unscaled harmonic B3LYP/6-31G(d,p) frequencies
[b]After correction for translational, rotational and vibrational energies determined at the B3LYP/6-31G(d,p) level

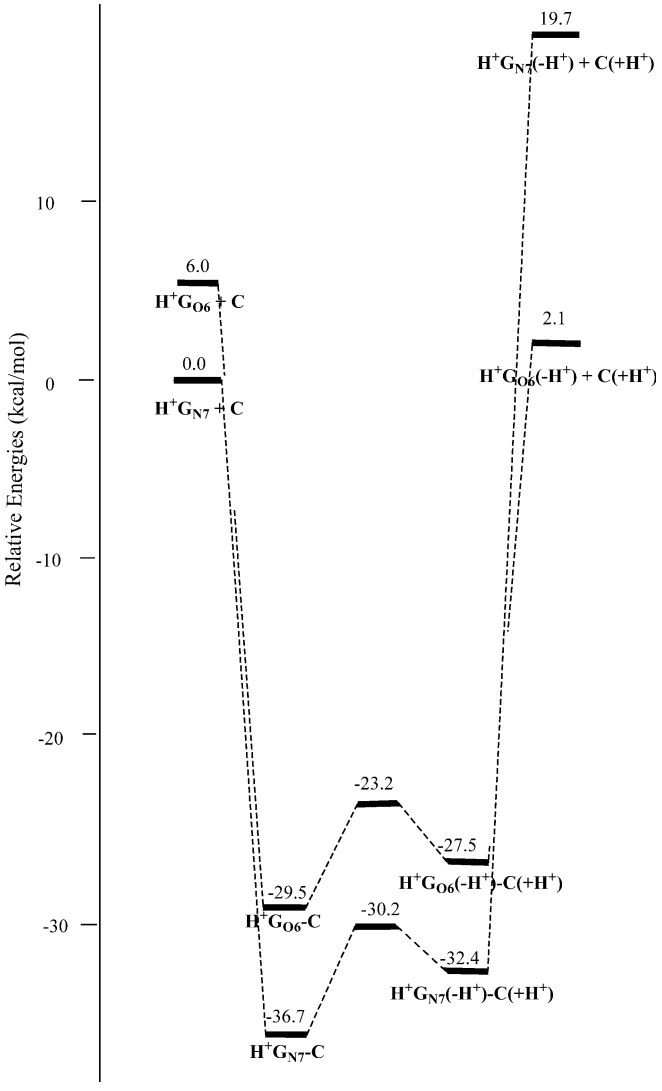

Fig. 5. Energy profile for the single N1–N3 proton transfer in N7- and O6-protonated systems in the gas phase

significantly smaller than those obtained at the AM1 level (11.8 and 8.2 kcal/mol) [42].

The behaviour of the protonated species is very different from that of the neutral base pair, for which the ion-pair formation, derived from the single-proton-transferred reaction, is found to be clearly unfavourable in the gas phase. In contrast, for the protonated systems, this reaction becomes a more favourable process owing to the increased acidity of guanine and to the fact that it does not imply the creation of charges but the transfer of a positive charge.

Important differences in the asymptotic behaviour of the two protonated systems can be observed in Fig. 5. Although some of the thermodynamic concepts that will be used in the discussion (such as proton affinity or exothermicity) correspond to enthalpy values, for simplicity and because relative thermodynamic corrections are small, we will refer to the potential-energy values given in Fig. 5. It can be observed that whereas the $H^+G_{N7}+C \rightarrow H^+G_{N7}(-H^+)+C(+H^+)$ reaction is strongly endothermic, the $H^+G_{O6}+C \rightarrow H^+G_{O6}(-H^+)+C(+H^+)$ reaction is slightly exothermic. The value of the reaction energy comes from two factors: the difference between cytosine N3 and guanine N7 or O6 proton affinities and the different stability of the two guanine tautomers [guanine and $H^+G_{N7}(-H^+)$ or guanine and $H^+G_{O6}(-H^+)$]. In the case of the N7-protonated system, the first factor is not of great importance, since both proton affinities are similar [22, 27, 32]. Therefore, in this case the guanine and $H^+G_{N7}(-H^+)$ tautomer stability determines the reaction energy. At the present level of theory, the relative energy of the two tautomers is 18.9 kcal/mol, in good agreement with recently published values [20, 35]. For the O6-protonated system the situation is different. The proton affinity of guanine at O6 is 5.1 kcal/mol smaller than that of cytosine at N3, whereas the energy difference between the corresponding tautomers [guanine and $H^+G_{O6}(-H^+)$] is only 1.3 kcal/mol. Thus, the exothermicity (−3.9 kcal/mol) arises from the larger proton affinity of cytosine.

The difference in the N7 and O6 proton-transferred asymptotes arises from the different stability of the two $H^+G_{N7}(-H^+)$ and $H^+G_{O6}(-H^+)$ tautomers, which is computed to be 17.6 kcal/mol. The less stable $H^+G_{N7}(-H^+)$ tautomer has a certain zwitterionic character, the positive charge mainly lying at the five-membered ring and the negative charge at the six-membered ring. This fact as well as the nature of the protonation site make N1 and O6 more basic in $H^+G_{N7}(-H^+)$ than in $H^+G_{O6}(-H^+)$ and so it is not surprising that hydrogen bonds in $H^+G_{N7}(-H^+)$–$C(+H^+)$ become stronger than in $H^+G_{O6}(-H^+)$–$C(+H^+)$. Note that the $H^+G(-H^+)$–$C(+H^+)$ interaction energy is significantly larger for the N7-protonated system (52.1 kcal/mol) than for the O6 one (29.6 kcal/mol), in agreement with the much shorter hydrogen-bond distances found for $H^+G_{N7}(-H^+)$–$C(+H^+)$ (see earlier).

In agreement with recently published results [20, 35], the dipole moments of the $H^+G_{N7}(-H^+)$ and $H^+G_{O6}(-H^+)$ tautomers are significantly different: 9.5 D for $H^+G_{N7}(-H^+)$ and 3.8 D for $H^+G_{O6}(-H^+)$. Thus, solvent effects may have an important role in determining the relative energies of the two tautomers. Indeed, the energy difference between $H^+G_{N7}(-H^+)$ and $H^+G_{O6}(-H^+)$ decreases from 17.6 to 9.8 kcal/mol.

The energy profiles obtained from single-point PCM calculations at the gas-phase geometries are shown in Fig. 6. Inclusion of solvent effects enhances the stability of the proton-transferred structure, especially for the O6-protonated system for which $H^+G_{O6}(-H^+)$–$C(+H^+)$ becomes stabler than $H^+G_{O6}C$ by 2.6 kcal/mol. In addition, in this case the energy barrier of the reaction decreases to 4.9 kcal/mol. Thus, solvent effects make the process even more favourable. As expected, the base-pair interaction energies in solution are smaller than in the gas phase mainly owing to desolvation effects produced in the formation of the complex. This is especially remarkable for $H^+G_{O6}(-H^+)$–$C(+H^+)$, which lies only 0.2 kcal/mol lower than its asymptote. Overall the $H^+G_{O6}+C \rightarrow H^+G_{O6}(-H^+)+C(+H^+)$ becomes more exothermic (−9.5 kcal/mol). The $H^+G_{N7}+C \rightarrow H^+G_{N7}(-H^+)+C(+H^+)$ reaction remains endothermic but only by 8.7 kcal/mol.

Such different asymptotic behaviour between O6- and N7-protonated systems has obviously different implications in mutagenic processes. Protonation at the O6 site of guanine–cytosine will very easily lead to the formation of an enol tautomer of guanine and protonated cytosine. Consequently rare tautomers will be introduced that could disturb the genetic code. In contrast, the formation of rare tautomers by protonation at N7 of guanine–cytosine will be much less probable. Nevertheless, considering that the proton affinity of G–C at O6 is 8.4 kcal/mol smaller than at N7, the population of H^+G_{O6}–C species will be much smaller than that of

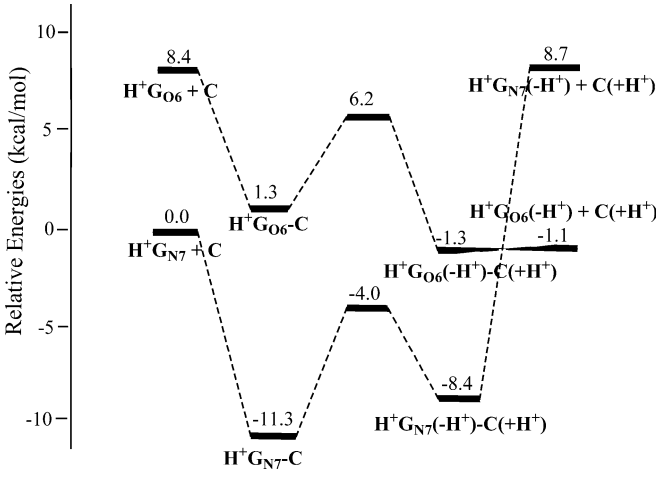

Fig. 6. Energy profile for the single N1–N3 proton transfer in N7- and O6-protonated systems obtained from polarized continuum model calculations considering water as the solvent

H^+G_{N7}–C species and, thus, the consequences of protonation at O6 will only be especially important in a nonequilibrium situation.

Conclusions

Intermolecular proton-transfer processes in neutral and protonated guanine–cytosine Watson–Crick base pairs have been studied using the B3LYP/6-31 + + G(d,p) method. Gas-phase calculations for the neutral system show that the double-proton-transfer reaction occurs through a concerted mechanism. However, PCM calculations seem to indicate that in solution the existence of the ion-pair intermediate cannot be disregarded. In any case, rare tautomeric products are clearly destabilized with respect to the canonical base pair, which suggests that proton-transfer reactions in uncharged base pairs will have small implications.

Protonation at the N7 and O6 sites of guanine favours the N1–N3 single-proton-transfer reaction. However, the double-proton-transfer process does not take place. This is in contrast to the neutral system, for which the double-proton-transferred structure is the only minimum found in the gas phase. This is due to the fact that for the protonated system the single-proton-transfer reaction does not imply the creation of an ion pair but just the transfer of a positive charge.

The major differences between the N7- and O6-protonated systems arise from the proton-transfer asymptote. For O6, the formation of an enol form of guanine and protonated cytosine is a very favourable process, whereas for N7 the reaction is energetically unfavourable. However, since protonation at N7 is more efficient than at O6, mutagenic effects will only be significant in a nonequilibrium situation or at very low pHs which are far from a physiological medium.

Acknowledgements. Financial support from MCYT and FEDER (project BQU2002–04112-C02–01), Departament d'Universitats, Recerca i Societat de la Informació (DURSI) (project 2001SGR-00182) and the use of the computational facilities of the Catalonia Supercomputer Center are gratefully acknowledged. M.S. is indebted to the DURSI of the Generalitat de Catalunya for financial support.

References

1. Watson JD, Crick FHC (1953) Nature 171:737
2. Löwdin PO (1963) Rev Mod Phys 35:724
3. Löwdin PO (1966) Adv Quantum Chem 2:213
4. Kwiatkowski JS, Bartlett RJ, Person WB (1988) J Am Chem Soc 110:2353
5. Szczesniak M, Szczepaniak K, Kwiatkowski JS, KuBulat K, Person WB (1988) J Am Chem Soc 110:8319
6. Les A, Adamowicz L, Bartlett RJ (1989) J Phys Chem 93:4001
7. Stewart EL, Foley CK, Allinger NL, Bowen JP (1994) J Am Chem Soc 116:7282
8. Gould IR, Burton NA, Hall RJ, Hillier IH (1995) J Mol Struct (THEOCHEM) 331:147
9. Colominas C, Luque FJ, Orozco M (1996) J Am Chem Soc 118:6811
10. Fogarasi G (1997) J Mol Struct 413–414:271
11. Leszczynski J (1998) J Phys Chem A 102:2357
12. Kobayashi R (1998) J Phys Chem A 102:10813
13. Ha TK, Keller HJ Gunde R, Gunthard HH (1999) J Phys Chem A 103:6612
14. Civcir PÜ (2000) J Mol Struct (THEOCHEM) 532:157
15. Sambrano JR, Souza AR, Queralt JJ, Andrés J (2000) Chem Phys Lett 317:437
16. Tian SX, Xu KZ (2001) Chem Phys 264:187
17. Fogarasi G (2002) J Phys Chem A 106:1381
18. Trygubenko SA, Bogdan TV, Rueda M, Orozco M, Luque FJ, Sponer J, Slavicek P, Hobza P (2002) Phys Chem Chem Phys 4:4192
19. Mons M, Dimicoli I, Piuzzi F, Tardivel B, Elhanine M. (2002) J Phys Chem A 106:5088
20. Hanus M, Ryjácek F, Kabelác M, Kubar T, Bogdan TV, Trygubenko SA, Hobza P (2003) J Am Chem Soc 125:7678
21. Lias SG, Liebmann JF, Levin RD (1984) J Phys Chem Ref Data 13:695
22. Greco F, Liguori A, Sindona G, Uccella N (1990) J Am Chem Soc 112:9092
23. Rodgers MT, Campbell S, Marzluff EM, Beauchamp JL (1995) Int J Mass Spectrom Ion Processes 148:1
24. Florián J, Baumruk V, Leszczynski J (1996) J Phys Chem 100:5578
25. Kampf G, Kapinos LE, Griesser R, Lippert B, Sigel H (2002) J Chem Soc Perkin Trans 2 1320
26. Bene JED (1983) J Phys Chem 87:367
27. Smets J, Houben L, Schoone K, Maes G, Adamowicz L (1996) Chem Phys Lett 262:789
28. Russo N, Toscano M, Grand A, Jolibois F (1998) J Comput Chem 19:989
29. Chandra AK, Nguyen MT, Uchimaru T, Zeegers-Huyskens, T (1999) J Phys Chem A 103:8853
30. Chandra AK, Nguyen MT, Zeegers-Huyskens T (2000) J Mol Struct (THEOCHEM) 519:1
31. Podolyan Y, Gorb L, Leszczynski J (2000) J Phys Chem A 104:7346
32. Stanks JR, Boerth DW (2002) In: 224th ACS national meeting. American Chemical Society, Washington, DC
33. Giese B, McNaughton D (2002) Phys Chem Chem Phys 4:5161
34. Huang Y, Kenttämaa H (2003) J Phys Chem A 107:4893
35. Jang YH, Goddard WA III, Noyes KT, Sowers LC, Hwang S, Chung DS (2003) J Phys Chem B 107:344
36. Kong YS, John MS, Löwdin PO (1987) Int J Quantum Chem Quantum Biol Symp 14:189
37. Clementi E (1972) Proc Natl Acad Sci USA 69:2942
38. Florián J, Leszczynski J (1996) J Am Chem Soc 118:3010
39. Hutter M, Clark T (1996) J Am Chem Soc 118:7574
40. Bertran J, Oliva A, Rodíguez-Santiago L, Sodupe M (1998) J Am Chem Soc 120:8159
41. Colson A-O, Besler B, Sevilla MD (1992) J Phys Chem 96:9787
42. Ford GP, Wang B (1992) Int J Quantum Chem 44:587
43. Bertran J, Noguera M, Sodupe M (2002) Afinidad 59:470
44. Becke AD (1993) J Chem Phys 98:5648
45. Lee C, Yang W, Parr RG (1988) Phys Rev B 37:785
46. Frisch MJ, Trucks GW, Schlegel HB, Scuseria GE, Robb MA, Cheesman JR, Zakrzewsky VG, Montgomery JA, Stratmann RE, Burant JC, Dapprich S, Millam JM, Daniels AD, Kudin KN, Strain MC, Farkas O, Tomasi J, Barone V, Cossi M, Cammi R, Mennucci B, Pomelli C, Adamo C, Clifford S, Ochterski J, Petersson GA, Ayala PY, Cui Q, Morokuma K, Malik DK, Rabuck AD, Raghavachari K, Foresman JB, Cioslowsky J, Ortiz JV, Baboul AG, Stefanov B, Liu G, Liashenko A, Piskorz P, Komaromi I, Gomperts R, Martin RL, Fox DJ, Keith TA, Al-Laham MA, Peng CY, Nanayakkara A, Gonzalez C, Challacombe M, Gill PMW, Johnson BG, Chen W, Wong MW, Andrés JL, Gonzalez C, Head-Gordon M, Replogle ES, Pople J.A (1998) Gaussian 98. Gaussian, Pittsburgh, PA
47. Hariharan PC, Pople JA (1973) Theor Chim Acta 28:213
48. Latajka Z, Bouteiller Y (1994) J Chem Phys 101:9793

49. Lee C, Fitzgerald G, Planas M, Novoa JJ (1996) J Phys Chem 100:7398
50. McQuarrie D (1986) Statistical mechanics. Harper and Row, New York
51. Weinhold F, Carpenter JE (1988) The structure of small molecules and ions. Plenum, New York
52. Reed AE, Curtiss LA, Weinhold F (1988) Chem Rev 88:899
53. Miertus S, Scrocco E, Tomasi J (1981) Chem Phys 55:17
54. Miertus S, Tomasi J (1982) Chem Phys 65:239
55. Cossi M, Barone V, Cammi R, Tomasi J (1996) Chem Phys Lett 255:327
56. Saenger W (1984) Principles of nucleic acid structure. Springer, Berlin Heidelberg New York, pp 123–124
57. Gould IR, Kollman PA (1994) J Am Chem Soc 116:2493
58. Santamaria R, Vázquez A (1994) J Comput Chem 9:981
59. Guerra CF, Bickelhaupt M, Snijders JG, Baerends EJ (2000) J Am Chem Soc 122:4117
60. Sponer J, Leszczynski J, Hobza P (1996) J Phys Chem 100:1965